Advances in Carrier Aggregation and Multi- User MIMO for LTE-Advanced:
Outcomes from SAMURAI project

Biljana BADIC[1], Andrea F. CATTONI[2], Michael DIEUDONNE[3], Jonathan DUPLICY[3], Peter FAZEKAS[4], Florian KALTENBERGER[5], István Z. KOVÁCS[6], Guillaume VIVIER[7],

[1]Intel Comneon GmbH, Suedwestpark 2-4, 90449 Nuremberg, Germany,
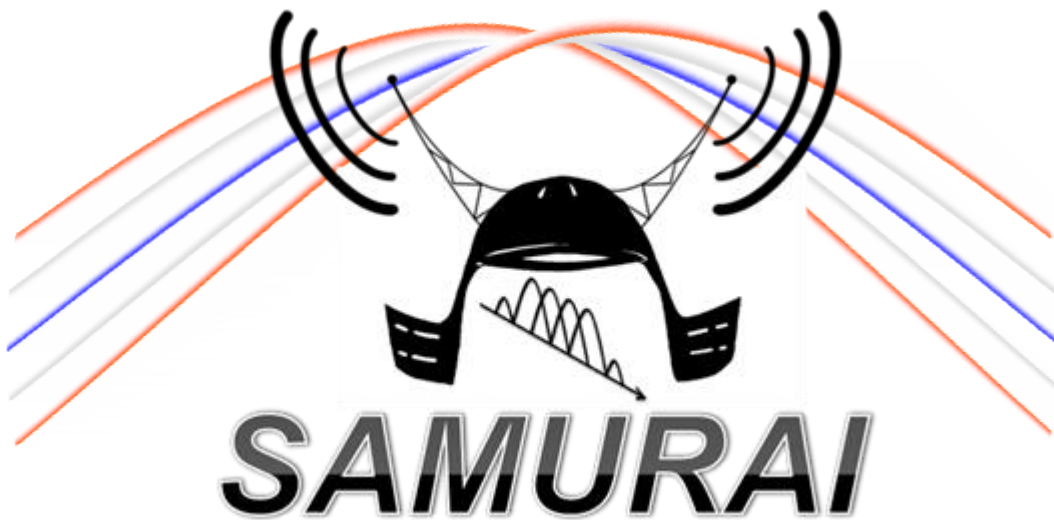[2]Department of Electronics System Aalborg University, 12 Niels Jernes Vej 12, 9220 Aalborg, Denmark,
[3]Agilent Technologies Laboratories, Wingepark 51, 3110 Rotselaar, Belgium,
[4]Department of Broadband Infocommunications, Budapest University of Technology and Economics, Goldmann Gyorgy ter 3, 1111 Budapest, Hungary,
[5]Eurecom, 2229 route des Crêtes, B.P.193, 06904 Sophia Antipolis Cedex, France,
[6]Nokia Siemens Networks Denmark A/S, Niels Jernes Vej 10, 9220 Aalborg, Denmark
[7]Sequans Communications, 19, Le Parvis de la Défense, 92 073 Paris La Défense Cedex, France

1. Executive Summary

To address dramatic increase of the demand for mobile broadband services and to support wider transmissions bandwidths, 3GPP Long Term Evolution (LTE) standard has introduced two powerful techniques, Multi User MIMO (MU-MIMO) and Carrier Aggregation (CA). The SAMURAI (Spectrum Aggregation and MUlti-user MIMO: ReAl-World Impact) project concentrated on the practical aspects of these two techniques and their development in LTE and LTE-Advanced systems. This white paper summarises the main outcomes of the project with particular emphasis of on the last phase of project, namely practical development and real-time evaluation of MU-MIMO and CA schemes. This means that the paper shows realistic considerations from hardware implementation point of view, as well as presents performance results under realistic assumptions.

The paper starts with highlighting the current standardisation status in MU-MIMO and CA. Then, invented MU-MIMO and CA algorithms and tools for their implementation are described in details. The SAMURAI interference aware receiver structure for MU-MIMO with an applicable link to system interfacing solution, that allows the evaluation of this receiver at system level is explained in detail. System level results showed that up to 20% gain in cell throughput is achievable by using the interference aware receiver, at the expense of some loss in the cell edge throughput performance. The white paper also describes in detail the implementation of this receiver algorithm in proof of concept hardware platform.

Realistic practical investigation of the implementation questions of CA from UE perspective are also shown in this white paper. The study presented in this paper reveals the main issues from testing and measurement point of view, namely in the area of wideband signal generation and spectrum analysis. System level performance results are also presented, revealing that using downlink CA practically doubles UE performance in case of modest load conditions. The emulation of the behaviour of multipath fading channel is an important area, for implementing measurement devices enabling the testing of UE and base station elements in realistic circumstances. During the project, new test and measurement needs are identified and solutions discussed with focus on increased bandwidth and channel emulation. The outcomes of SAMURAI project allow the reproduction of MIMO channel, for subsequent testing and measurement purposes. An important aspect of this work is that it allows the modelling and emulation of channel behaviour taking into account the spatial component of the channel. The results of this work will likely appear in future testing and measurement devices.

One of the most exciting questions is the performance of joint application of MU-MIMO and CA transmission schemes in the network. Practical considerations on the implementation issues at the UE, network and test equipment side are analysed in the white paper. Besides this qualitative analysis, network level performance results of both schemes applied jointly are presented. From the investigation outcome, it can be observed that under heavy load conditions applying MU-MIMO together with CA compensates for the relatively modest gains that would be achievable by CA only. With applying proper scheduling and adaptive SU/MU-MIMO switching, the scheme can provide up to 20% gain in average UE throughput performance, compared to the case when only SU-MIMO with CA is used. In the uplink direction, results show that in terms of average user throughput, more than 50% gain is achievable compared to the CA scheme, when CA is extended by multi-cluster scheduling and MU-MIMO.

This paper also shows the hardware proof of concept platforms that are (at least partially) direct results of the SAMURAI project. The OpenAirInterface platform was mainly extended by MU-MIMO transmission schemes. The ASGARD platform was mostly developed in the framework of the project and is used for implementation of Autonomous Component Carrier Selection algorithm.

Finally, the paper also includes recommendations to research and industrial bodies on how to exploit the tools and findings originated from the project. Possible future research directions in MU-MIMO and CA fields are also pointed out. It can be stated that these future directions, as well as results and main recommendations rising from future research are greatly dependent on the details of schemes that will be part of LTE Release 11 and 12.

The paper is organised as follows: Section 2 gives a short overview of the way MU-MIMO and CA schemes are / planned to be included in the 3GPP LTE releases. Section 3 and Section 4 detailed analysis and performance analysis of MU-MIMO and CA developments within SAMURAI. In Section 5 advantages and disadvantages for employing and combining these two features are explored. Real world impacts and recommendations from SAMURAI projects are given in Section 0and finally, Section 0 concludes the paper.

2. Introduction

Wireless data usage is increasing faster than ever before. Smartphones and broadband-enabled portables, such as laptops or tablets, are now seeing high penetration in many markets, and the superior user experience offered by such devices has led to exponential growth of mobile data traffic. These large capacity demands can be met only by highly efficient and optimized mobile network infrastructures. Significant improvements are expected with the ongoing rollout of OFDMA- (Orthogonal Frequency Division Multiple Access-) based networks: IEEE 802.16x (WiMAX) and 3GPP (3rd Generation Partnership Project) LTE. Among others, two key technologies are considered in the to-be-deployed upcoming versions of these networks (WiMAX Evolution and LTE-Advanced): Multi-user MIMO (MU-MIMO) and carrier aggregation (CA) (or initially named Spectrum Aggregation (SA)).

The SAMURAI (Spectrum Aggregation and MUlti-user MIMO: ReAl-World Impact) project has had as objective the study of these two technologies in real-world conditions. While appealing in theory, their performance may differ in practice and the return on investment for their deployment may not be sufficient for operators.

As for MU-MIMO, it is fundamental to understand the increased complexity involved the effects of errors in channel estimation / feedback as well as the effect of the remaining multi-user (MU) interference.

As for carrier aggregation, the increased complexity (power consumption, multiple RF chains, etc), scheduling, backward compatibility and interference management aspects deserve proper studies and real-world experimentations.

2.1 3GPP standardisation status

2.1.1 MU-MIMO

MU-MIMO is already supported in 3GPP LTE Release 8 with a 4 bit (in case of 4 transmit antennas) codebook feedback based precoding transmission mode 5 (TM5). Single User MIMO (SU-MIMO) and MU-MIMO use the same codebook for precoding but the codebook has been optimized for SU-MIMO case and therefore is suboptimal for MU-MIMO. Thus, the performance of stand-alone Rel-8 MU-MIMO is inferior to Rel-8 SU-MIMO transmission mode 4 (TM4) or UE specific reference signal (RS) based beamforming (BF) transmission mode 7 (TM7). This suboptimal codebook selection limits the gains of multi-user transmission and thereby the practical implementation of MU-MIMO systems.

In LTE Release 9, two streams of UE specific RS are supported for MU-MIMO transmission in the downlink dual-layer beamforming (DLBF) transmission mode 8 (TM8). The TM8 has been defined which includes both SU and MU-MIMO transmission capabilities without the need for the UEs to be reconfigured via higher layer signalling when switching between SU and MU mode on the shared data channel. DLBF is supported by a single transmission mode that utilizes code division multiplexing (CDM) - multiplexed demodulation reference signals (DM-RS) transmitted on two user-specific antenna ports. The possible configurations from network side are dual-layer transmission, single-layer transmission without co-channel transmission on another layer, and single-layer transmission with co-channel transmission on another layer. Dynamic indication on which of the two UE specific antenna ports is used is supported. However, there is no explicit signalling of the presence/absence of a co-scheduled UE on the same resources, i.e. the UE does not know whether interlayer interference exists or not.

In LTE-Advanced, Release10, new transmission mode 9 (TM9) was introduced allowing 'seamless' switching between SU and MU mode. Configurations with up to 8 x 8 MIMO antennas are to be supported and set of precoding codebooks is extended accordingly. For configurations with 8 transmit antennas a dual-codebook approach is used and up to four UEs can be scheduled for MU-MIMO transmission. The precoding applied is the dual-codebook approach. This configuration provides good performance in both high and low spatial correlation channels. Additionally to user specific DM-RS introduced in Rel-9, new channel state information RS (CSI-RS) have been introduced in Rel-10.

2.1.2 Carrier Aggregation

Carrier aggregation is a key feature that has been introduced into the Release 10 version of LTE specifications. CA is supported for FDD and TDD, and is used to support bandwidths larger than 20 MHz by the simultaneous transmission of multiple component carriers in parallel to/from the same UE. CA is introduced in LTE-Adv in order to increase peak and average throughput, and cell-edge user throughput efficiency. As suggested by ITU-R, the maximum bandwidth being targeted is 100 MHz. Obviously this is limited by practical deployment scenarios and eNB/UE (Base Station/User Equipment) RF implementation. Component carriers do not have to be contiguous in frequency and can even be located in different frequency bands in order to enable exploitation of fragmented spectrum allocations. This latter point has turned out to be even more important in practice (for operators) than total contiguous bandwidths beyond 20 MHz (no such spectrum available). Increased flexibility is also an important

driver for CA (possibly bigger than increased peak data rates), allowing for fast load sharing between carriers and frequency dependent scheduling. CA also provides higher peak data rate for coverage-limited UEs with wideband transmission, though in uplink this may not be the case due to power limitations. Finally, one use case being envisioned is providing interference coordination in heterogeneous network deployments involving e.g. uncoordinated co-channel deployment of home eNBs. While multiple component carriers are needed, this does not necessarily require support for carrier aggregation (i.e. the terminal capability of aggregating carriers).

We refer the reader to [1] for details around layer 1 and 2 aspects for LTE-A as well as an outlook on Release 11.

3. MU-MIMO developments in SAMURAI

Multi-user MIMO is a key feature of LTE and LTE Advanced. In theory it provides throughput gains that scale linearly with the number of antennas at the eNB. In practice however, several problems remain, such as the residual multi-user interference seen at the UE. In SAMURAI, a novel interference aware (IA) receiver architecture was developed to tackle this problem. The main ideas behind this algorithm and some link-level simulation results are described in Section 3.1. Section 3.2 studies the effect of this receiver algorithm on a system level. To this end, a novel link-to-system interface has been developed. Further, a proof-of-concept of the IA receiver has been developed based on the OpenAirInterface LTE experimentation platform and is described in Section 3.3. Last but not least we highlight another aspect of MU-MIMO in Section 3.4, namely channel modeling and emulation. We conclude with a summary of the key achievements in Section 3.5.

3.1 Interference aware receivers algorithms

The interference-aware (IA) receiver is a key feature for high throughput MU-MIMO transmission in LTE Systems. Contrary to a simple interference-unaware (IU) receiver, which considers the interference to be unknown and hence treats it as noise, the IA receiver exploits the known interference structure to increase its detection reliability. In the following, we give a more detailed explanation of the MU-MIMO scenario motivating the necessity of an IA receiver design and describe its functionality.

3.1.1 Motivation

In the MU-MIMO scenario the base-station uses its antennas to transmit independent data streams to multiple non-cooperative users. For instance, in LTE Release 8 the MU-MIMO transmission scenario is defined in TM5, where an eNB with two transmit antennas serves two users. The key difference to SU-MIMO is the fact that the users are spatially separated and do not cooperate. This separation has advantages as well as drawbacks. An advantage is that the channels of both users tend to be less correlated which is referred to as multi-user diversity gain. The drawback is that the inter-user interference experienced by the UEs cannot be processed jointly at the receive side and thus no efficient interference mitigation is possible. Without efficient interference management the benefits of MU-MIMO cannot be realized. In theory, the interference management, through techniques such as zero-forcing precoding, can be carried out by the eNB if downlink channel estimates are available at the eNB. However, the required high-quality channel estimates at the eNB are very difficult to obtain in practice which is why TM5 LTE Release. 8 defines a simple codebook-based precoding scheme. Although this precoding scheme can reduce the inter-user interference, e.g. through efficient scheduling algorithms, there may still be a significant amount of interference experienced by the users. Therefore, a key challenge to achieve the MU-MIMO gains in LTE systems lies in the capability of the UEs to efficiently cancel the interference.

3.1.2 Functionality

Due to the precoding operation at the eNB, each user receives a linear combination of his data stream and the interfering data stream. To efficiently cancel the interference, the user needs to know the characteristics of the interference, more precisely, the interfering channel, precoding vector and symbol constellation. The interfering channel is identical to the desired channel since both desired signal and interference are part of the same transmit signal and pass through the same channel. Moreover, the precoding vector of the interfering stream can be implied since it is orthogonal to the desired precoding vector and defined in the common codebook. The only information unavailable to the UE is the interfering symbol constellation which can either be QPSK, 16QAM or 64QAM. The interfering symbol constellation could be estimated by observing the statistical properties of the received signal but the current assumption is that both desired and interfering symbol constellations, are identical. It has also been shown that a false assumption on the interfering symbol constellation decreases the performance only slightly [8].

The receiver computes the log-likelihood ratios (LLRs), i.e., a measure for each bit indicating if the particular bit is more likely to be zero or one. The LLRs are computed for every bit in the codeword and are the input to the channel decoder. The

computation of the LLRs is based on the classical maximum a-posteriori probability (MAP) criterion with max-Log approximation. In particular, the IA receiver computes the LLRs under the assumption of a specific constellation for the interfering symbol. Detailed expressions of the LLR expressions can be found in [8].

3.1.3   Link-level simulation results

Here we compare IA detector explained in previous section with an IRC receiver and a low-complexity, single-user, linear MMSE (LMMSE) detector for the downlink MU-MIMO LTE Release 8. The effect of feedback delay, channel estimation, and spatial correlation has been considered in the investigation. For the link-level evaluation, the parameters defined in Table 1have been assumed.

Due to the straightforward implementation, Least-Squares (LS) channel estimation technique has been applied in investigation. The results are shown in Figure 3-1 - Figure 3-3. Block error rate (BLER) is presented as a function of the average SNR in dB. For comparison, LTE TM4, SU-MIMO with the ratio of

Parameters	Settings
Test Scenario	3GPP Macro cell case 1, 19 sites, 57 cells with 3 center cells simulated
Number of UEs	20 UEs per cell and all 20 UEs are semi-statically allocated in MU-MIMO mode when MU-MIMO transmission is configured
Carrier frequency and simulated bandwidth	10 MHz bandwidth centered at 2 GHz
Packet scheduling	Proportional fair in both time and frequency domain
1st BLER target	10%
Tx and Rx transmission scheme	2x2 and 4x2 MIMO with SU and MU configured
Tx Correlation	Alt 1: Uncorrelated with 4λ Tx antennas separation and 15° azimuth spread
	Alt 2: Correlated with 0.5λ Tx antennas separation and 8° azimuth spread
MU-MIMO precoding	Unitary precoder as used in SU-MIMO LTE Release 8
Minimum supported data rate in MU-MIMO mode T_{min}	64 kbps
UE MU Receiver type	LMMSE, IRC and IA max-log MAP
Feedback type	Per subband CQI and Wideband PMI Feedback (One PMI for the whole bandwidth)
Feedback delay	0 TTI and 8 TTI delay
Channel models	urban micro channel model (uncorrelated) and urban macro (correlated)

Table 1 LTE parameters used in investigation

PDSCH (Physical Downlink Shared Channel) EPRE (Energy Per Resource Element) to cell-specific RS EPRE of −3dB is shown as a reference scenario.

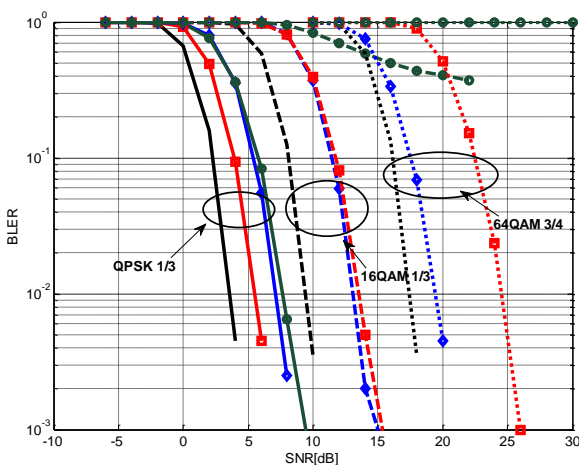Figure 3-1 illustrates the performance of all

Figure 3-1 MU-MIMO performance in urban micro (uncorrelated) channels, 30km/h velocity and no feedback delay for various modulation orders and receivers (black solid: SU-MIMO, red: IRC, blue: IA receiver, green: LLMSE

considered detectors for QPSK 1/3, 16QAM 1/3 and 64QAM, 3/4 in uncorrelated channels. The performance of the LMMSE detector degrades with increasing modulation order. For QPSK, IRC slightly outperforms IA max-log MAP (Maximum A Posteriori) detector. However, for 64QAM IA significantly outperforms IRC by almost 5 dB at 10−2 BLER. This can be explained by the fact that IA detector exploits not only the interference structure but also performs joint detection as it is aware of the modulation from the interfering user.

The joint effect of feedback delay and channel correlation is illustrated for 16QAM and IA detectors in Figure 3-2 - Figure 3-3. In uncorrelated channels (Figure 3-2), the feedback delay results in up to 2 dB loss at 10^{-2} BLER. However, in the case of high channel correlation, the corresponding performance is reduced by up to 5 dB at 10^{-2} BLER for feedback delay of 8 TTIs (transmit time interval) as shown in Figure 3-3.
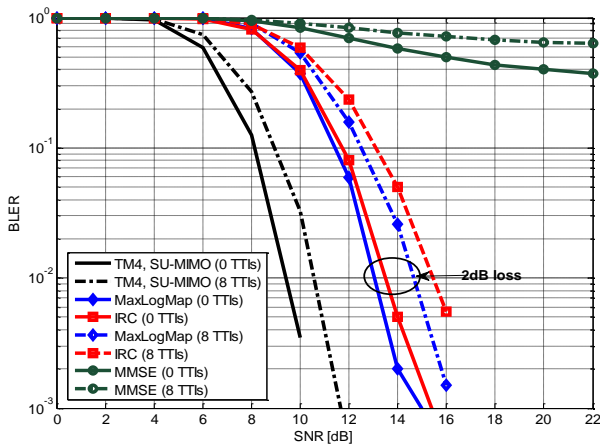
Figure 3-2 MU-MIMO performance in urban micro (uncorrelated) channels, 30km/h velocity, LM channel estimation, feedback delay for 16QAM and various receivers
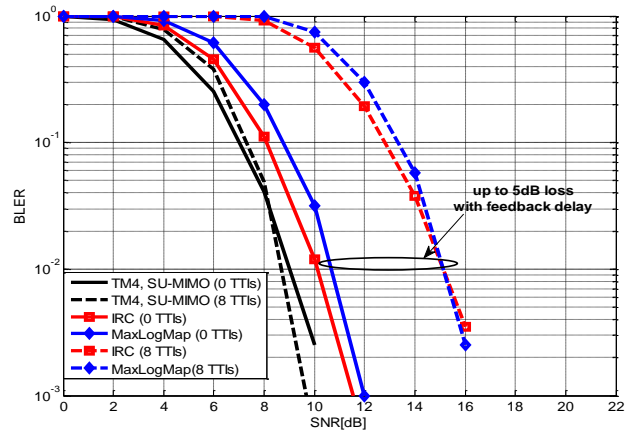

Figure 3-3 MU-MIMO performance in urban macro (correlated) channels, 30km/h velocity, LM channel estimation, feedback delay for 16QAM and various receivers

The results shown here demonstrate the possible gains of IA receivers and indicate that the interference aware type of receivers are good candidates for the practical implementation in MU-MIMO LTE systems. It has been shown that one can obtain the best overall performance with the IA max-log MAP detector if the modulation of the paired UEs is known. However, additional control information bits dedicated to this modulation update may not be desirable as they will increase the downlink overhead and not comparable with the current standardization. By doing a smart scheduling, it is possible to indicate what type of modulation is used for the paired UEs without having dedicated overhead bits for this purpose. The UEs are always informed which MCS will be applied to the next transmitted data packet. In the pairing and selection process, we can then select or force the secondary UEs to have the same modulation as the primary one. More results can be found in project deliverable [2] and references therein.

3.2 System level studies

3.2.1 A link-to-system interface for the interference aware receiver

In order to study the performance of the IA receiver on a system level, first link-to-system interface needs to be developed. State-of-the-art link to system interfacing or link abstraction schemes include effective SINR mapping (EESM) and mutual information based effective SINR mapping (MIESM). These two methods differ in the way the varying SINRs of a codeword are compressed and mapped to an effective SINR value. This value is then used to read the equivalent BLER from the AWGN performance curves of a particular modulation and code scheme (MCS).

For the IA receiver it turns out that the MIESM method is by far the more suitable method in terms of mean squared error, complexity, and calibration effort. The method is based on the mutual information expressions of an interference channel. Details of the method can be found in [9] and [10].

3.2.2 System level simulation

The goal of these studies was to disclose the potential system-level gain which can be obtained when IA receivers are used for MU-MIMO reception compared to the rank-adaptive SU-MIMO transmission references. The reader should note that these studies *did not* aim to show absolute system performance numbers or to investigate SU-MIMO performance, as compared to the reference 3GPP LTE/LTE-A MIMO evaluation studies.

The system-level simulations settings, parameters and scheduling algorithm used can be found it the above referenced documents. A downlink 2x2 MIMO transmission setup was used with 10MHz system bandwidth at 2 GHz carrier frequency. The 3GPP typical urban deployment and ITU based geometric channel model were employed. The main difference compared to the previous studies was due to the limitation of the available link-to-system interface mapping curves, which included only QPSK and 16QAM modulation and coding sets. Therefore, to provide a fair comparison, we have used the same QPSK and 16QAM MCS sets in all simulations presented in the following. All UE terminals simulated are assumed to have the same MIMO capability and implement the IA receiver algorithm. Furthermore, in these evaluations only the full buffer traffic model (UE download data continuously) has been used in order to have sufficient user diversity in the system. The three simulation sets to be compared are:

"MU-MIMO Ideal IA": Rank-adaptive SU-MIMO combined with rank-1 MU-MIMO using ideal IA receiver (zero residual MU interference at UE), and ideal MU-MIMO CQI compensation at the eNB

"MU-MIMO MIESM-IA": Rank-adaptive SU-MIMO combined with rank-1 MU-MIMO using realistic IA receiver, based on the MIESM L2SI curves, and ideal CQI compensation at the eNB

"SU-MIMO": Rank-adaptive SU-MIMO

3.2.3   Results and discussions

Figure 3-4 shows the main system level performance metrics obtained from the MU-MIMO IA evaluations along with the reference SU-MIMO results, in terms of average cell throughput and UE throughput statistics. Compared to the ideal case of using ideal MU IA (zero residual MU interference at the UE) the results for the MIESM-IA show very good performance and

only 3% degradation; the MIESM IA yields an overall cell throughput gain of approx. 20% compared to reference SU-MIMO transmission case. Furthermore, looking at the UE throughput statistics, it is clear that this gain comes at the cost of sacrificing the cell-edge performance, with a loss of approximately 35% compared to the SU-MIMO case.

shows more in-sight into the cell throughput gain mechanisms in these studies, in terms of the achieved system throughput vs. Geometry factor. It is evident from these results that MU-MIMO transmission schemes can take advantage of the high G-factor (good SINR conditions at the UE) hence improves the overall system spectral efficiency. A second observation is that UEs in low-medium G-factor conditions are better scheduled in SU-MIMO mode due to the rank-adaptation.
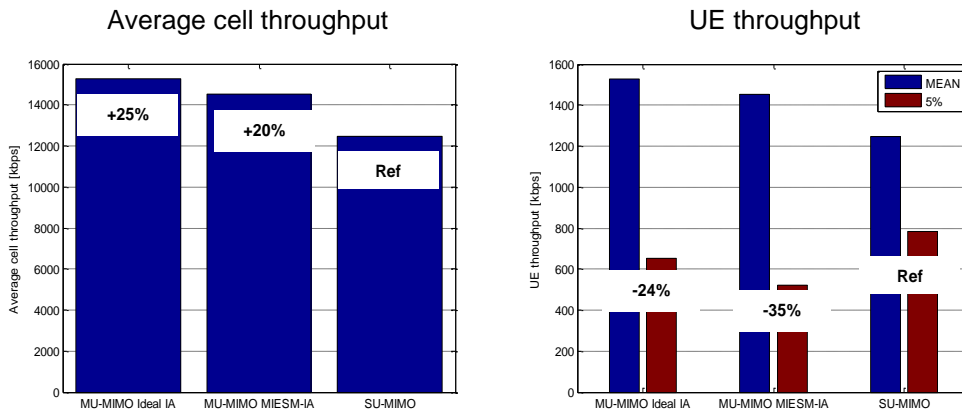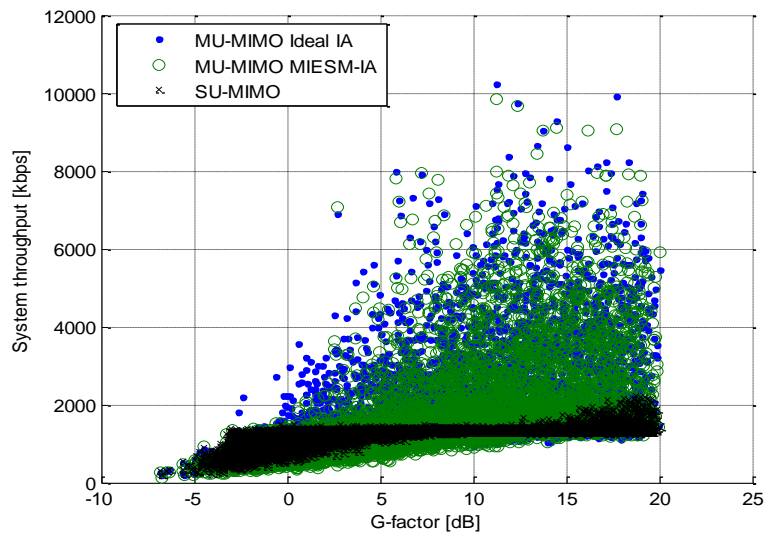

Figure   3-4   System-level performance metrics from the MU-MIMO IA receiver evaluation studies. A downlink 2x2 MIMO transmission setup was used with 10MHz system bandwidth at 2 GHz carrier frequency.

Figure 3-5 System-level cell throughput versus Geometry factor from the MU-MIMO IA receiver evaluation studies.

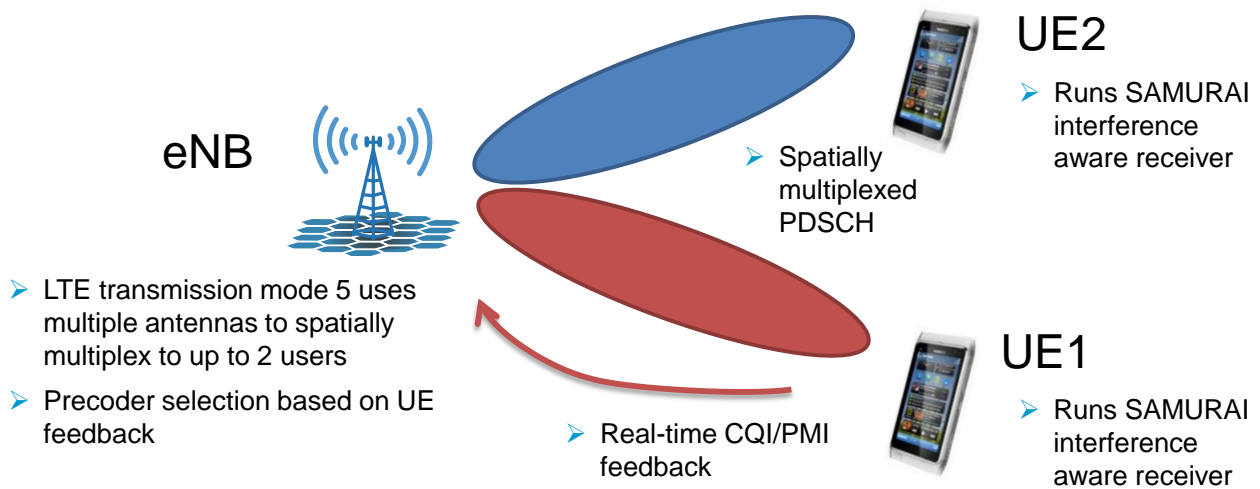## 3.3 Proof of Concept and Platform Implementation

Figure 3-6 Overview of the MU-MIMO Proof-of-concept

One of the main goals is demonstrate the benefits of the IA receiver over the IU receiver architecture in a realistic LTE Release 8 setting. We choose a setup as depicted in Figure 3-6 with one eNB and two UEs. The eNB has two antennas, while the two UEs have one antenna each. The two UEs provide real-time feedback (subband PMI, wideband CQI) and implement the IA receiver. Based on the feedback, the eNB schedules orthogonal users for simultaneous downlink transmissions. We have introduced a new DCI format 1E instead of the format 1D defined in LTE Release 8. This was necessary to allow for per sub-band PMI feedback in order to compare to TM6, where a per-sub-band PMI feedback is specified.

As a hardware platform we have used the Express MIMO boards together with the LIME RF frontend. Express MIMO is a baseband processing board, which comprises two FPGAs: one Xilinx XC5VLX330 for real-time embedded signal processing applications and one Xilinx XC5VLX110T for control. The card uses an eight-way PCI express interface to communicate with the host PC. The card employs four high-speed A/D and D/A converters from Analog Devices (AD9832) allowing to drive four RF chains using quadrature modulation. In the current setting the ADAC are configured to 7.68 MSPS (corresponding to the LTE 5MHz bandwidth allocation). As an RF front-end we have used a custom design based on the LMS6002D evaluation boards from Lime Microsystems. Up to four such front-ends can be connected, each independently tunable from 300 MHz to 3.8 GHz with a maximum output power of 0dBm. However, the current filters limit the carrier frequency to the band around 1.9GHz. As an example a UE is depicted in Figure 3-7.
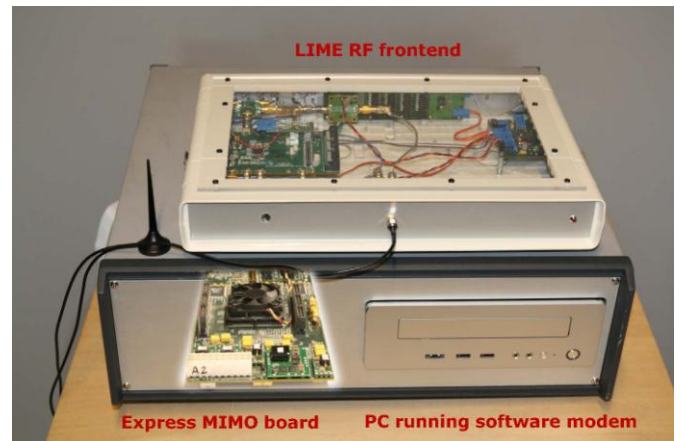

Figure 3-7: OpenAirInterface UE

3.4 Channel modeling and emulation for MU-MIMO

3.4.1 Deterministic fading

Until recently, channel emulation was associated solely with stochastic models. Based on measurements, the scientific community has derived various randomness-based models to mimic different kinds of environments. These models do not reflect any particular scene, but by sweeping through their statistics will give a good idea of the average DUT performance. Rayleigh, Rice, Nagakami are such typical models and are supported by the Agilent PXB and Agilent System Vue. Conformance tests are based on these stochastic models. However these tests actually fail to guarantee any satisfactory performance in the field. In addition, with MIMO and closed-loop schemes being part of new standards, the importance of channel emulation is growing and appeals for closer-to-reality channel emulation for accurate testing.

Geometrical models (like the WINNER model) have been proposed recently. They offer interesting capabilities in particular with respect to the spatial dimension (MIMO) but like the above models they are still based on statistical distributions and are not meant to mimic any particular area.

The test industry has recently understood the needs for "real-world" emulation and started two years ago to release some solutions. The common denominator between the solutions is the "replay from file" feature. Basically, the time-variant (vector, in the MIMO case) channel impulse response is stored in a file and replayed. The channel being fully characterized by the file, no randomness is involved hence the naming "deterministic fading".

3.4.2   Raygen – the channel data preprocessor

Our objective in this context is the development of a channel preprocessing tool for the Agilent PXB channel emulator. The main function of this tool is to serve as an interface/conversion tool between the PXB channel fading engine and a ray-tracing simulator. Ray-tracing software predicts the propagation of radio waves based on the phenomena of reflection, refraction, diffraction, and absorption (attenuation). In an urbanized area, for instance, the propagation is mostly affected by reflections from buildings and objects. The actual ray data preprocessing is performed upfront, i. e., on a non-real-time basis. The key feature of this tool is to enable for the PXB channel emulator the previously described functionality to deterministically "store & replay" a given channel. The benefits are a more realistic reflection of the RF channel in the context of spatial trajectories and movement, perfect test repeatability, and increased test flexibility.
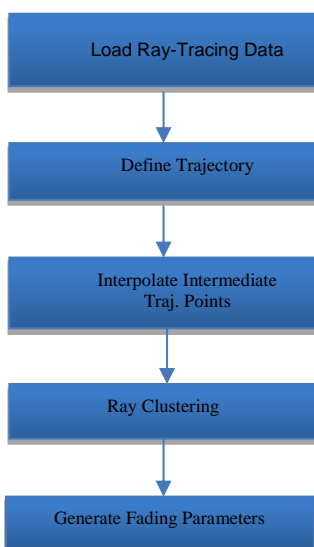

Figure 3-8: Raygen process flow.

In the first stage of the process the channel preprocessor tool, from here on referred to as Raygen, loads and parses ray data from a ray-tracing

simulator and creates a snapshot grid. The complete process flow is given in Figure 3-8. Each snapshot on the grid is defined by a number of predicted wave propagation paths, called rays. The visualization of loaded rays for a specific reception point on the snapshot grid is demonstrated in Figure 3-9. Rays are characterized by their propagation delay, complex coefficient (path-loss and carrier-to-interference ratio), angle of departure (azimuth and elevation), angle of arrival (azimuth and elevation), and interaction points in the given topographic area. This representation is also called double-directional impulse response (DDIR). Furthermore, this stage involves the removal of zero-ray snapshots, the addition of virtual line-of-sight (LOS), and discarding unwanted rays (based on excess delay threshold and dynamic range threshold). An example of a DDIR is given in Figure 3-10.
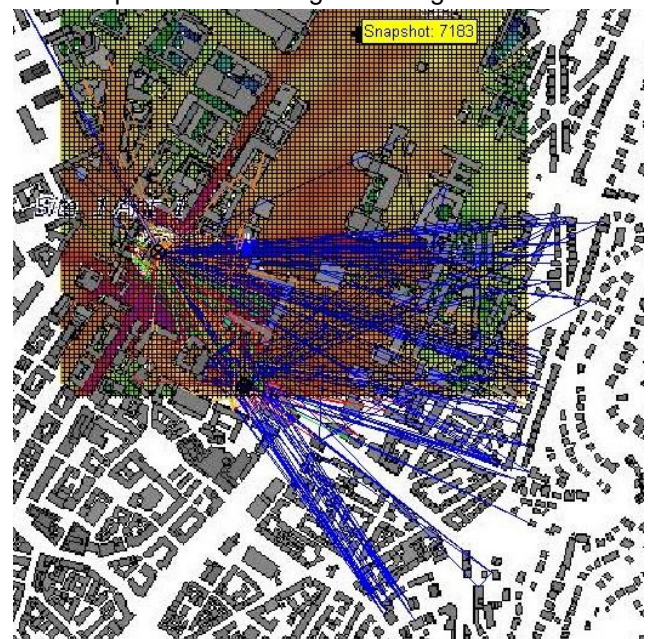

Figure 3-9: Visualization of ray tracing data in an urbanized zone (top view).
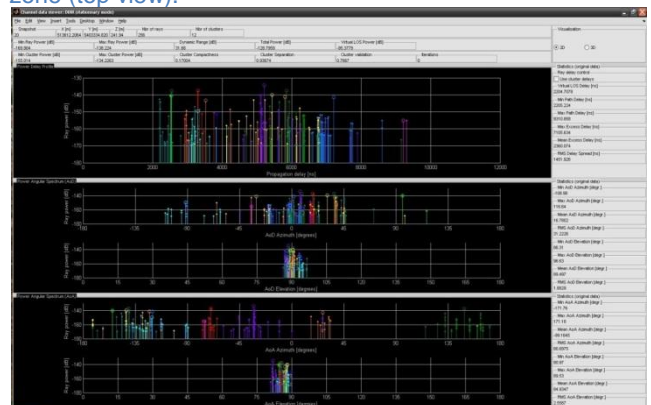

Figure 3-10: Snapshot DDIR visualization, from top: propagation delay, AoD azimuth and elevation, AoA azimuth and elevation.

The deterministic fading functionality involving ray-tracing data and a channel emulator can also be viewed as drive test reconstruction in the laboratory. For that reason the next stage comprises the definition (by drawing) of a trajectory. An important

feature in this process is giving the user feedback about the relationship between the created trajectory and the loaded snapshot grid, and what might be the possible impact on the emulation. This feedback is achieved by means of a live computation of various metrics such as emulation time, emulation distance, RMS trajectory-to-grid distance, RMS channel-update deviation distance (the deviation caused by updating the channel fading parameters at fixed time intervals), etc. The number of trajectory segments is determined by the maximum segment distance and the maximum relative segment angle. The trajectory creation process is shown in Figure 3-11.
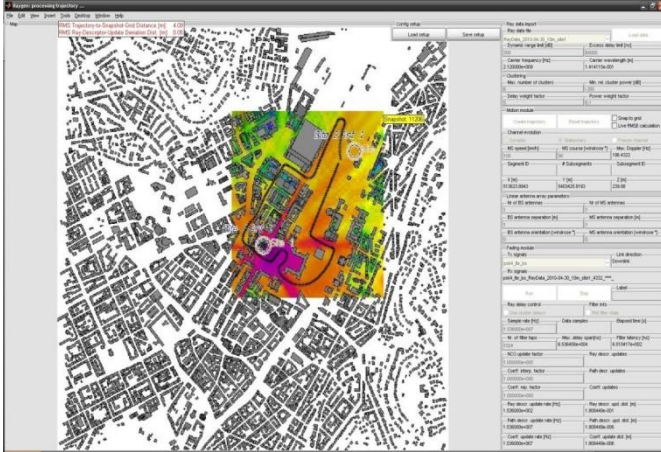

Figure 3-11: Trajectory definition in the Raygen tool

Wireless channel will vary in time based on the movement over a trajectory. Luckily, the fading parameters do not have to vary as fast as the signal sampling rate (F_s). In theory, the rate should be at least twice the maximum Doppler shift (F_d), nevertheless a higher update rate is generally recommended in practice. This shift is proportional to the speed of the mobile (v) and the carrier frequency (F_c) and defined as (c being the speed of light):

$$F_d = F_c \frac{v}{c}$$

However, the update rate of fading parameters (in the sense of spatial movement) typically highly exceeds the density of the snapshot grid. Common snapshot grid density is 2-10 m. The obvious solution for this issue is the introduction of intermediate points to the trajectory segments and spatial interpolation of the channel parameters (DDIRs) at these points. For any two given neighbouring snapshots on the trajectory we initiate a ray-to-ray mapping based on the multi-path component distances (MCD) between rays. MCD in this case depends on the inter-ray difference in AoA, delay, and power. The optimal assignment/mapping is achieved by the Hungarian algorithm (published by H. Kuhn, 1955). Since the sets of rays in snapshots are, in general, completely independent, a certain amount of rays will be too distant and will remain unmapped. Given the ray-to-ray mapping, the intermediate (artificial) snapshots

will be created by inverse distance weighted interpolation of the two neighboring ray sets.

Channel impulse response in the PXB is modeled using a tapped delay line implementation. Tapped delay line is a traditional technique for emulating a fading channel. In these models, each "tap" represents the sum of numerous multipath signals arriving at the same time. The tap amplitudes typically decrease over time as the signals arriving at later times have larger path loss and possibly undergo multiple reflections from the surrounding environment. PXB uses 24 taps in this model which is also the upper limit for distinct delayed paths that can be fed to the emulator from the Raygen tool. On the other hand, the number of rays per snapshot is normally higher (e. g., 256 rays). This difference triggers the need for clustering the rays in a snapshot into 24 (or less) clusters and eventually replacing the rays by their cluster-sum equivalent. The clustering is also based on MCD among rays in a particular snapshot. Nevertheless, the MCD definitions in these two stages might vary, since for optimal performance it may be necessary to adapt them (e. g. discarding power as a distance factor for clustering).

The last stage of the process is the generation of fading parameters at the appropriate rate, saving them to a file, and uploading them to the channel emulator. Given DDIRs for all points (including the interpolated intermediate ones) on a trajectory, we translate the T_x and R_x antenna offsets and extract a set of ray descriptors for each MIMO branch for all the points. Besides ray delay, magnitude, and phase, the ray descriptors include also the ray Doppler shift parameter. In the next step the ray descriptors are converted to so-called path descriptors, which means the incorporation of the ray Doppler shift into the path (I,Q) coefficients and upsampling to the required PXB-channel-update rate. The last task is to perform (ray/)path descriptor recombination according to obtained ray-cluster assignment.

The channel fading requirements on the memory storage can be easily computed as follows:

$$\frac{\#byte}{s} = M.\,N.\,24.\,16B.\,K.\,F_d$$

M and N are the numbers of T_x and R_x antennas, respectively, 24 is the number of filter taps in the PXB, and 16 bytes is the assumed size of one path descriptor. K is the oversampling factor with respect to the max Doppler (frequency) shift F_d.

Assuming a MIMO 2x2 system, at a carrier frequency of 1.8GHz, a UE moving at 30m/s and an oversampling factor of 24, this gives a storage requirement of 6.64MB/s, i.e., 1GB for 150 seconds of emulation. The update rate of path descriptors in this example is 4.32 kHz, which is typically much less than the transmission sampling rate.

3.4.3 Conclusions and lessons learned

A software pre-processor able to convert deterministic data into a readable format for the PXB channel emulator has been developed. The work done in the frame of SAMURAI will enable the reproducibility of any MIMO channel taking into account its spatial component. The limitation of the current platform have been identified and documented for a possible future upgrade. Agilent intends to exploit the result in products in the next years.

3.5 Key achievements

One of the major achievements of SAMURAI with respect to MU-MIMO is the proof of concept that the interference aware receiver developed within the project significantly alleviates the problem of multi-user interference in MU-MIMO systems. The receiver was studied on a link level and on a system level thanks to the newly developed link-to-system interface and it showed remarkable performance improvements on both levels. Furthermore, the receiver was implemented and tested successfully on the OpenAirInterface software defined radio platform, where it is used in an LTE Rel. 8 MU-MIMO scenario. Last but not least, SAMURAI also made a significant contribution to the MU-MIMO channel emulator from Agilent by integration realistic ray-tracing results in the channel model.

4. CA developments in SAMURAI

4.1 Carrier aggregation challenges in the device

In this section we browse a panorama of the challenges related to the implementation of carrier aggregation in an user terminal.

The 3GPP standardization has defined up to 40 bands, with two duplex mode, FDD and TDD, multiple duplex gaps from 30MHz to 400MHz, various widths, various specific requirements due to regional context and various channelization (from 1.4MHz to 20MHz). It is already complicated to design a device able to support most of these bands to enable global roaming.

Carrier aggregation adds up complexity by allowing the possibility to aggregate multiple bands in various manners: intra-band aggregation, contiguous or non-contiguous; inter-band aggregation. An initial challenge is thus to design a RF front-end able to support all the possible band arrangements. Similarly, the certification of such device becomes very complex because of the exponential number of test cases that has to be defined due to the combinatorial growth of bands and band arrangements.

An RF front end consists in everything between the antenna and the base band processor. It includes antenna, filters, switches, du- or di-plexer power
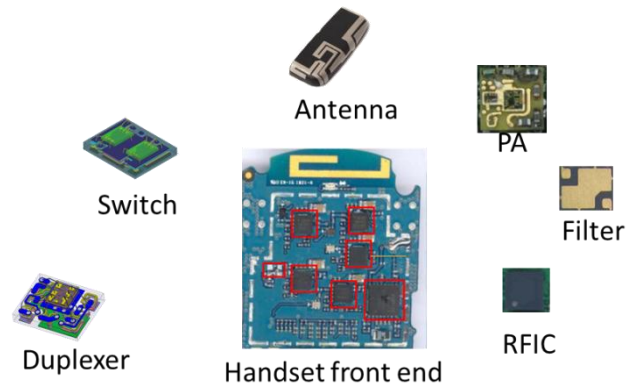

Figure 4-1 Main components of a RF front-end.

amplifier and the transceiver (the RFIC) as illustrated by the Figure 4-1.

The impact of carrier aggregation on the Front-end design is straightforward. The required number of receiver chain increases with the number of component carriers. More filters, more switches are required, yielding to an increase of the insertion losses and definitely to a higher cost of the complete solution. To avoid a "simple" duplication of the Rx chains smarter components component can be used which is not straightforward as illustrated by the twofold examples:

- **Antenna.** In nowadays smartphones, antennas already fill all the empty space (if any). Indeed, a smartphone is supposed to be multi-bands and multi-modes. It has to be 2G and 3G, to support WiFi and GPS and sometimes acts as a FM radio or even Digital Video Broadcast receiver. All these systems require their own antennas since they operate in different bands. Isolation between technology should be ensured to avoid pollution for instance of your 3G connection by your local WiFi link. Moreover, the recent wireless systems use MIMO techniques which by definition require de-correlated antennas for a given band. Adding up carrier aggregation, the number of antenna has to be more or less doubled whilst the device size cannot increase. The way forward is to consider wide band antennas and/or active antenna systems, able to tune the antenna response to the required frequency band. Such active system could perform active matching or play on the antenna pattern to do Tx or Rx beamforming.

- **PA:** Power amplifiers amplify the radiated signal. They are mostly characterized by their efficiency and their linearity. Unfortunately, multi-band PA often suffers from poor efficiency. Therefore, to support UL carrier aggregation it is almost mandatory to double the transmit chain and the PA (except the specific case of intra-band CA, for which the use of a single chain may be sufficient).

Doubling the Tx chain has a direct impact on the cost of the device and on its power consumption. CA has thus a direct impact on the UE design. Within SAMURAI we focused on the case of intra-band CA, which would be a simpler case from the RF front-end standpoint. However, such case still raises some issues at the base band level, especially if the contiguous carriers are misaligned. We have investigated the impact of such misalignment and concluded to the fact that it is equivalent to the generation of spurs in the Rx chain, including possible frequency drift in the spectrum. We have investigated methods to mitigate such spurs by for instance removing the subcarriers on which they are detected. Such approaches were simulated and implemented on a prototype. Results show that the performance degradation due to the spurs was almost fully mitigated when applying the proposed method.

In SAMURAI we have investigated the technical issues at the base band and RF-Front end levels to bring the carrier aggregation capability. Several challenges were identified and some promising techniques were proposed to overcome some of these challenges. Although all barriers are not yet cleared, the project allowed a good progress towards smart and efficient implementation of CA in an user terminal.

4.2 Test and measurement aspects for carrier aggregation

This sections cover the advance made in Samurai around the test of carrier aggregated transmitter and receivers.

4.2.1 Signal generation test platform

We discuss here the management of generating several carriers from the test equipment point of view. The device under test (DUT) is the UE under CA scenario in this context. Signal generation can be managed by using different configurations of hardware and software test-platform setups. This is because the complex CA scenarios (inter-band/intra-band contiguous/non-contiguous CC) cannot be tested adequately by any high-end single test equipment available in the market today. The SAMURAI employed UE test platform involves multiple test instruments, such as signal generators, synchronization equipment, RF up-converters, RF splitters and couplers, with significant customization in both hardware and software.

Contiguous or close to contiguous signals are the simplest case. The platform has only one transmission chain which consists of one signal generator with associated software module, a channel emulation platform and an RF up-converter followed by an output interface to the DUT. We assume that the DUT has only one receiver chain and it can

process at most two contiguous CCs at a time. The setup facilitates the measurement of error vector magnitude (EVM), and block error rate (BLER) for receiver testing.

In order to test the non-contiguous CA scenarios (multiple CCs operating at different bands), a setup consisting of multiple signal generators can be configured where each signal generator represents a CC (or a set of contiguous CCs) for one operating band. The non–contiguous CCs are directly fed to the different receiver branches of the DUT. There are two common setups to configure multiple signal generators for UE testing, i.e., with and without RF phase coherence.

The major disadvantage of using multiple instrument solution is that the final setup includes besides multiple signal generators also multiple other components. The user has to carefully manage all the components adequately along with the synchronization requirements. A more convenient option is to use advanced systems that have inbuilt multiple signal generators along with channel emulator platforms and provide adequate synchronization between all the components (see Figure 4-2). Such instruments provide interfaces to multiple RF up-converters through the input/output digital card outlets. These input/output cards can be directly accessed either by the DSPs meant for baseband signal generation or by the DSPs meant for channel faders. Since it is possible to sum either the outputs of the signal generators or the faders, the instrument can be set into various pre-configured setups.

4.2.2 Wider band spectrum analysis

With LTE-A and carrier aggregation, the RF span goes towards greater values. This can go potentially over 1GHz, e.g., with a chunk in the 800MHz and another one in the 1.8GHz. Obviously, the analysis of such a scheme will be conducted with two separate analyzers. For smaller spans, however, one may wish to perform the analysis in a single box; first to reduce the costs and second to ease the synchronization between the bands.
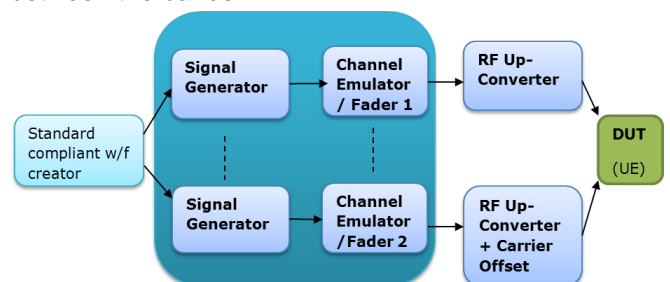

Figure 4-2: Advanced solution with inbuilt general purpose multiple signal generators

In the following we discuss the spectrum analysis with instantaneous bandwidth in excess of 200 MHz,

specifically a combination of Agilent instruments and analysis capabilities in a measurement setup in order to achieve signal and spectrum analysis at 250 MHz instantaneous analysis bandwidth. It is important to note that currently the best state-of-the-art, commercially available single-box spectrum analyser (Agilent's PXA – Performance Spectrum Analyzer) provides up to 160 MHz analysis bandwidth.

Figure 4-3 shows the architecture of Agilent's 250 MHz bandwidth PXI-based Vector Signal Analyzer. This is a signal analyzer which is built up modularly with PXI cards. We use this block diagram as a representative example to discuss the overall structure of a wideband signal analyzer. Each block in the figure represents a separate card.

One of the benefits of FFT-based spectrum analysis is that the performance of the spectrum analyzer can be tailored according to the needs for resolution bandwidth and dynamic range. This is achieved by windowing the input signal in the appropriate way prior to FFT processing. Rectangular window gives the smallest possible resolution bandwidth, but establishes a relatively high leakage. The Hanning window has a wider main lobe, but sidelobes get lower quickly. This is hence a better choice for measurements requiring a high dynamic range. The flattop window has the widest main lobe and hence a flat response over adjacent bins. This is hence a good choice when accurate amplitude estimation is important.
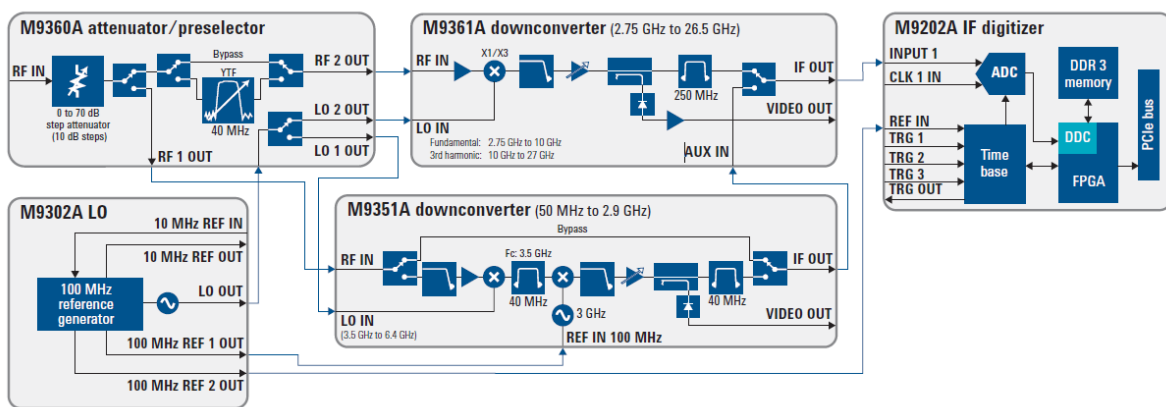

Figure 4-3: Overall 250 MHz signal analyzer block diagram

4.3 Downlink carrier aggregation: system level performance

Carrier aggregation is one of the main features specified in 3GPP LTE-Advanced (Release 10). The technique provides, in both downlink and uplink, mechanism to utilize several carriers simultaneously, hence increased capacity. A good overview of the 3GPP carrier aggregation can be found in [1].

As described in Section 4.1 and Section 4.2 downlink carrier aggregation can pose several challenges from RF implementation and T&M equipment point of view. Based on our SAMURAI studies we have evaluated these challenges and summarized them in Even though the standard specifications allow for many possible combinations [1] in practice a given operator has only a couple of choice available due to its available spectrum. In Table 2 we look at the most likely European/US operator scenario, at least for the first deployments and the next couple of years before new spectrum is made available by regulators.

In its simplest implementation, carrier aggregation is applied between two contiguous or non-contiguous carriers with same bandwidth transmitted in the same frequency band e.g., two carriers of 20 MHz each in the 2600 MHz band. Another option in LTE-Advanced

Release 10 is to aggregate two carriers from two different frequency bands e.g., one carrier from the 800 MHz band and one carrier from the 2100 MHz band, and not necessarily having the same bandwidth on the two carriers.

To illustrate the downlink system level performance gains when using contiguous intra-band carrier aggregation, in Figure 4-4 we show the estimated user throughput statistics for various offered load conditions. Both LTE Release 8 with 20 MHz bandwidth and LTE-Advanced with 2x20MHz carrier aggregation results are depicted. As expected, carrier aggregation can significantly boost the average and peak throughput for all LTE-Advanced capable terminals, especially in low load conditions.

From practical terminal equipment availability point of view, as detailed in Table 1, the contiguous intra-band carrier aggregation configuration is the most likely to be supported by the first generation LTE terminals. However, from network operator point of view, the inter-band carrier aggregation is the most feasible in the near term due to the available spectrum constraints and therefore more advanced terminal implementation solutions are required to take full advantage of this transmission technique. Although

Table 2 Carrier aggregation: a complexity vs. performance view on the most likely carrier configuration scenarios to be deployed in the first LTE-Advanced capable networks, with up to two carriers, each with 20MHz bandwidth.

		1 carrier (reference)	2 carriers contiguous intra-band	2 carriers non contiguous intra-band	2 carriers inter-band
Handset	**Support features**	1RF Front-End 1Rx chain	1RF Front-End 1 or 2 Rx chains	1 or 2 RF Front-End 2 Rx chains	2 RFIC or a dedicated CA one 2 front-ends Same BB as intra-band case
	Increased power consumption	Reference	For DL, power consumption is mostly driven by UE category For UL, adding a secondary CC would impact the power consumption (~2x in case of 2 PAs)		
Network	**Average downlink UE throughput gain**	0% LTE Rel'8 UE (20MHz)	80% - 100% LTE-A UE	80% - 100% LTE-A UE	70% - 80% LTE-A UE
	Required support features per antenna port	1 RF Front-End 1 Tx-Rx BB chain	1 RF Front-End 1 Tx-Rx BB chain	1 RF Front-End (≤80MHz total BW) 2 Tx-Rx BB chain	2 RF Front-End 2 Tx-Rx BB chain 2 antennas might be needed
Test & Measurements	**Increased complexity**	Reference	2x20MHz is easily covered by current signal generators and analyzers	Depending on the carrier frequency differences, may require two signal generators / analyzers in parallel with proper synchronization..	

not specifically detailed in our analysis above, the practicalities of implementing uplink carrier aggregation are similar to the downlink case with a notable difference with respect to the need for better UE power consumption management.
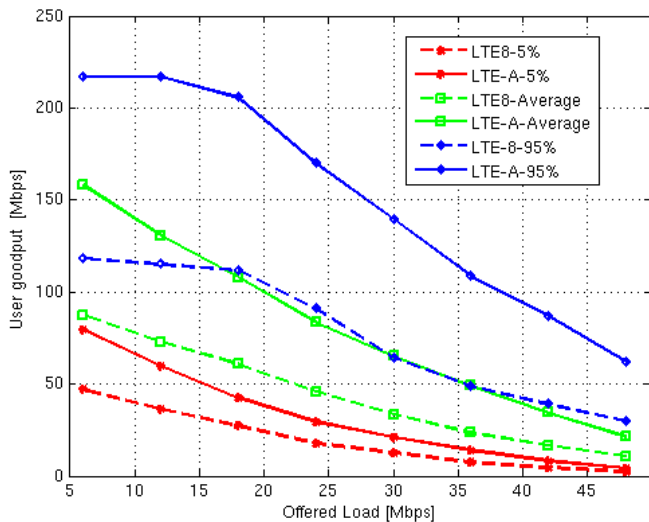

Figure 4-4 Downlink user throughout performance vs. traffic load for 2x20MHz contiguous intra-band carrier aggregation.

4.4 Key achievements

In the project SAMURAI we have investigated carrier aggregation at various levels: at the PHY and RF front end level and at the MAC and upper layers level. For the latter case, the CA brings to the radio resource management a new degree of freedom that would in theory allows to optimize the overall system capacity.

At the PHY and RF6 front end level, we have identified numerous challenges and proposed way forwards for some of them, covering not only the user equipment aspects but including the test equipment aspects.

At the MAC and upper layers level, we have evaluated the system level performance of using carrier aggregation. It appears that CA could significantly improve system performance, especially in context of low load scenario, assuming that enough CA able terminals would be present in the cell. More detailed results can be found in project deliverables [3] - [5].

5. LTE Advanced MU-MIMO and CA in Practice

In this section we explore the pros and cons for employing and combining the two LTE-Advanced features investigated in the SAMURAI project: carrier aggregation and Multi-user MIMO. We assume that both these transmission techniques are implemented by the network equipment and there are sufficient user equipment terminals in the network which can support these schemes. The rank-adaptive Single-user MIMO is assumed as baseline in LTE-Advanced

systems and our focus is on the benefits of Multi-user MIMO. Furthermore, only the currently standardized, LTE-Advanced intra-site carrier aggregation technique is analyzed. We note that the introduction of the 3GPP LTE Release 11-12 inter-site carrier aggregation features could significantly change the recommendation below and the questions need to be addressed as part of dedicated study.

5.1 Downlink MU-MIMO

Multi-user MIMO is one of the main transmission schemes specified in 3GPP LTE. The technique provides, in both downlink and uplink, mechanism to better utilize the available time-frequency resources by super-imposing transmission/reception to/from different user terminals in both time and frequency. A good overview of the 3GPP MU-MIMO can be found in [6]. Our focus in SAMURAI has been the investigation of downlink MU-MIMO schemes and user terminal algorithms (see Section 3). In Table 3 we have summarized the main benefits and identified requirements for downlink multi-user MIMO implementation.

In Figure 5-1 we show the estimated downlink cell performance gain when enabling LTE-Advanced MU-MIMO transmission and assuming the user terminals support (muti-user) interference aware receive algorithm. The achievable gain of 20-25% in average cell throughput comes at the price of a reduced cell-edge (95% cellcoverage) performance when MU-MIMO is used.

Therefore, in practical the use of downlink MU-MIMO has to be carefully planned and selectively enabled in a network based on cell load conditions and main key performance indicator target(s).Another practical aspect which needs to be considered is the requirement for a correlated antenna array with at least 4 antenna parts on the transmission side (base station) in order to maximize the gain from downlink MU-MIMO transmission.
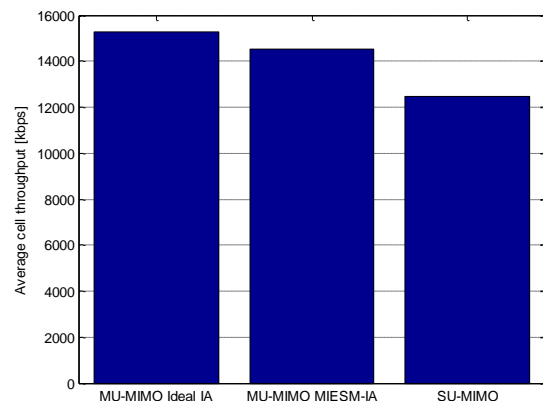

Figure 5-1 Estimated downlink cell performance gain for LTE-Advanced MU-MIMO transmission scheme when user terminals are employing a (multi-user) Interference Aware algorithm [3]. Full buffer traffic is assumed.

Table 3 Downlink Multi-user MIMO: a complexity vs. performance view.

	Receiver type	Single user MIMO	MU-MIMO LTE Release 8		MU-MIMO LTE-Advanced (Release 10)	
		MMSE	MMSE	Interference aware Rx	MMSE	Interference aware Rx
Handset	**Link level throughput**		0% (TM5)	Not supported	>25% * * scenario and feedback configuration dependent	
	Complexity	2 Rx antenna ports	Max 2 Rx antenna ports single layer	Not applicable	Max 4 Rx antenna ports, dual layer	
Network	**Average downlink cell throughput gain**	Reference	Up to 10%	Not applicable	Up to 15% (2 Rx antenna)	Up to 25% (2 Rx antenna)
	Required features	2 Tx antenna ports Standard BB processing Standard LTE TD-FDPS	4 Tx antenna ports (correlated antenna array) Standard BB processing Multi-user MIMO time-domain scheduling		4 Tx antenna ports (correlated antenna array) Increased BB processing due to larger system BW ≥ 20MHz Multi-user MIMO time-domain scheduling	
Test & Measurements	**Increased complexity**		Need proper MU-MIMO channel model and/or the generation of re-created MU interference that the receiver would face.			

Table 4 Recommended use scenarios for joint CA and MU-MIMO transmission in LTE-Advanced depending on the cell traffic load. The base stations are assumed to be equipped with a 4TX/RX antenna configuration and all user terminals using 1TX/2Rx antenna configuration. Two intra-band carriers of 20MHz are available for carrier aggregation.

	Low cell load	High cell load
Downlink CA	Rank-adaptive SU-MIMO (rank-2)	SU-MIMO/MU-MIMO rank-1
Uplink CA	Dual -cluster	Dual-cluster with SU-MIMO/ MU-MIMO rank-1

5.2 Benefits from combining CA and MU-MIMO

The SAMURAI studies have shown that the achievable system level gains for each of the two transmission techniques vary when the cell load is varied. Hence, a first analysis of the potential gains from combining CA and MU-MIMO can be readily made based on the load in the network, as shown in Table 4. One of the main conclusions from the MU-MIMO studies was that the technique offers visible system gains only when there is sufficient number of active user terminals in the serving cell i.e., a 'high load' needs to be served.

For both, downlink and uplink transmissions, the MU-MIMO techniques do not bring any additional gain when 'low load' situation is estimated in the cell. The performance in 'low load' situations can, however, be effectively improved with carrier aggregation technique combined with single-user MIMO transmission schemes in downlink or multi-cluster scheduling in uplink. In 'high load' scenarios, downlink MU-MIMO can provide additional gain and compensate for the lower gains provided by carrier aggregation. The actual performance depends heavily on the adopted scheduling solution for switching between single-user and multi-user MIMO transmissions. As a general guideline, we suggest using the MU-MIMO transmission up to a rank below the available SU-MIMO transmission rank (e.g. rank-1 in the Table 1). The average user throughput can be improved with up 20 % compared to using CA and SU-MIMO only. The results illustrating this conclusion are presented in Figure 5-3. In uplink, a multi-cluster and MU-MIMO scheduling can be effectively combined, and the MU-MIMO provides average user throughput improvements in the order of 30 % compared to the multi-cluster without MU-MIMO performance. Figure 5-3 illustrates our uplink conclusions.
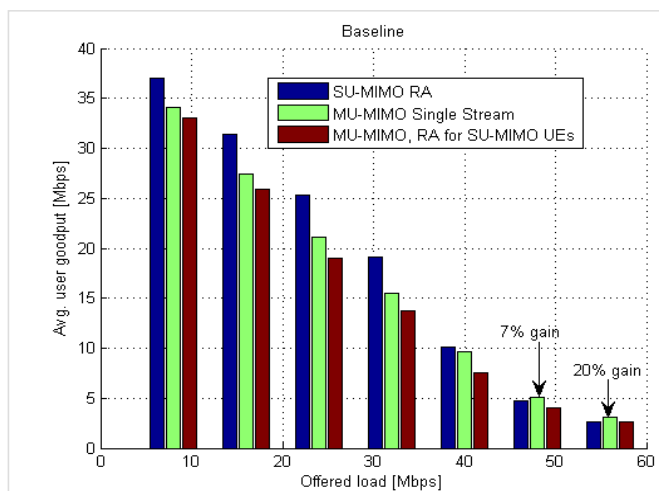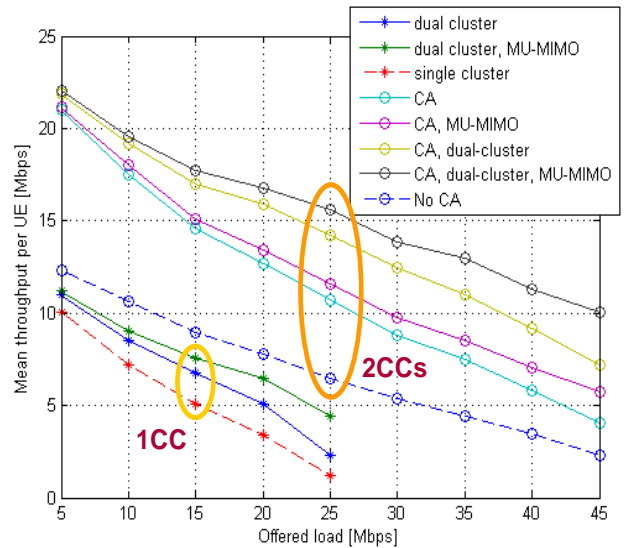
Figure 5-3 Uplink user throughput performance for combined CA and MU-MIMO transmission schemes.

6. Exploitation of results and tools available from SAMURAI

The SAMURAI consortium is composed by both academic and industrial partners. In both cases, the path for exploiting the SAMURAI results has been traced. The example can be then followed by other institutions and companies.

6.1 Academic exploitation

The SAMURAI results can be of course considered as state of the art literature that can be exploited at three main levels. The first one is of course advances in research, where engineer and researchers push forward the techniques developed in the project. The second level is the didactic at Ph.D. level. Advanced courses could use the material generated by SAMURAI as baseline and didactic examples from a research perspective. Finally, the usage of the knowledge in graduate and undergraduate courses could allow reaching higher educational points using the SAMURAI techniques in order to explain the modern wireless communications from an application-oriented perspective.

6.2 Industrial exploitation

The SAMURAI results are already expected to be incorporated in next generation base stations, mobile phone chipsets, and test and measurement products. Other companies, besides to the ones part of the consortium, can use the knowledge built by the SAMURAI project to drive their research in a more accurate direction. Furthermore, the SAMURAI project can be seen by mobile operators as a baseline investigation for identifying possible deployment advantages of MU-MIMO and CA.

6.3 Available tools from the SAMURAI project

Mainly two tools have been developed during the SAMURAI project. Such tools are:

Figure 5-2 Downlink user throughout performance for combined CA and MU-MIMO transmission schemes.

- OpenAirInterfaces: mainly developed by Eurecom, used within the SAMURAI project as demonstration platform for MU-MIMO and CA.
- ASGARD: mainly developed by Aalborg University, used in the SAMURAI project as demonstration platform for ACCS.

Both the tools have been made available to the scientific and industrial communities as a part of open development philosophies, in order to ensure that the SAMURAI contribution could be an essential part of future scientific and research studies.

6.3.1 OpenAirInterface

OpenAirInterface [11]-[13] is an open-source platform for experimentation in wireless systems with a strong focus on cellular technologies such as LTE and LTE-Advanced. The platform comprises both hardware and software components and can be used for simulation/emulation as well as real-time experimentation. It comprises the entire protocol stack from the physical to the networking layer. The objective of this platform is to fill the gap between the simulation and real experimentation by providing the baselines for protocol validation, performance evaluation and pre-deployment system test. The key features are

- Extensive LTE Release 8.6 compliance with some features from LTE-Advanced
- Full protocol stack for both UE and eNB implementations
- Provides Linux networking interface to run any application on top
- 4x4 MIMO with 20MHz bandwidth
- Carrier aggregation possible
- eNB output power 30dBm

OpenAirInterface comprises a highly optimised C/C++ implementation all of the elements of the 3GPP LTE Rel 8.6 protocol stack for UE and eNB (PHY, MAC, RLC, RRC, PDCP, NAS driver). Apart from real-time operation of the software modem on a hardware target, the full protocol stack can be run in emulation. The OpenAirInterface emulation environment allows for virtualization of network nodes within physical machines and distributed deployment on wired Ethernet networks. Nodes in the network communicate via direct-memory transfer when they are part of the same physical machine and via multicast IP over Ethernet when they are in different machines. In the first case the emulator can either be run with the full PHY layer or with PHY abstraction while in the latter case nodes interface at layer 2. The rest of the protocol stack (MAC and RLC) for each node instance uses the same implementation, as would the full system. Each node has its own IP interface that can be connected either to an application or a traffic generator. The emulator also comprises a simple mobility model and channel models including path loss, shadow fading and stochastic small scale fading.

6.3.2 ASGARD

The Application-oriented Software on General-purpose-processor for Advanced Radio Development (ASGARD) [11]- [13] is a software radio platform designed for fast prototyping of higher layer algorithms and medium/large scale test bed development. The software, written in C++, exploits the latest releases of open source libraries and free Linux distributions. The coding of the platform is based on the Test-Driven Development approach, allowing thorough extensive code testing the development of virtually bug-free code. The code runs on modern and multi-core general purpose processor machines, mounting Linux as operating system (even though compatibility is ensured only with Ubuntu Linux at the moment).

The platform is designed to virtually support any type of hardware. It currently operates in conjunction with the commercial-off-the-shelf software radio front end "Universal Software Radio Peripheral" (USRP) produced by Ettus Research [USRP]. This choice is due to the widespread usage of such device in the international research environment, even though it is mostly academic. The key strength of ASGARD resides in its flexibility and modularity. Any developed code is wrapped into small modules called "component" that virtually allow system designers and developers to build up any possible architecture. The components are joined together by flexible and dynamic communication modules that allow optimizing the information flow within the system. Furthermore, ASGARD provides full control over the multi-threading of the process. Expert users have then the tools for optimizing their desired architecture in a clean and clear way, without the need of tweaking or hacking the main design principles of the platform. These features make it possible to fast prototype any kind of higher layer algorithm, even though the original design has been thought for L3/L4 RRM ones. Physical layer processing has been foreseen in the development roadmap, thanks to the cooperation with Trinity College Dublin. The platform has also a server process that enables the centralized management of demonstration and experimentation activities. A graphical user interface for the SAMURAI ACCS demonstrator has been made available for providing a basic template methodology for personalized interfaces specific for the desired application. ASGARD is also designed to be user-friendly, allowing users to configure the system with human-readable XML files.

The code is open source, and it is released under a cooperative development license enforcing code sharing amongst ASGARD developer community.

Figure 6-1 small subset of the ASGARD-based testbed at Aalborg University

6.4 Open issues / potential future research work

The SAMURAI project covered quite extensively the topics that were focus of research, i.e. MU-MIMO and CA. Nevertheless, some issues are still open and will have to be tackled in the future in order to make the investigated techniques a commercial reality.

To some extent, SAMURAI investigated the multi-layer (ML) MU-MIMO schemes introduced in LTE Release 10. This implies that the introduction of user-specific reference symbol can cause additional interference issues in both channel estimation and receiver design. While the investigated methodologies have been assessed from the feasibility point of view, additional issues could rise in their practical implementation.

Test and measurement issues are mostly due to augmenting the one box tester (or base station emulator, used to test handsets or UE) with a MU-MIMO interference emulation capability. Today these machines maintain links with one handset only. Therefore, there is a need of adding interference generation capability to emulate a MU-MIMO signal as perceived by the UE in the field.

From the Carrier Aggregation side, SAMURAI has investigated the twofold aspects, namely what should be done on the terminal side to enable the CA features and how to benefit from CA capability at the system level side. On the latter aspect, CA will be initially used mostly in downlink and almost exclusively between a low carrier band and a high carrier band. The operators will likely have to configure their networks according to the expected load and coverage of all their available carriers. High traffic areas may need several carriers and more advanced carrier management also at SON level. The full benefits of CA at network level are strongly dependent on the type and number of terminals capable of CA available. On the implementation side, CA is not a straightforward feature for the terminal. The standard has introduced many possible combinations (intra or inter band, contiguous or non-contiguous), adding the complexity of the support of the already numerous bands defined in LTE, LTE-Advanced. From the RF and base band perspective numerous challenges are still opened to better integrate CA in the terminal, to maintain low cost, small size and low power solutions. One could say that CA is a first pragmatic step towards agile radio system and software definable radio.

The ACCS-like schemes are currently under investigation in 3GPP under the framework of Operational Carrier Selection (OCS) mechanisms. Several Autonomous (AOSC) proposals exist from various companies in 3GPP, with focus on macro-pico carrier management. It is still open how and when these mechanisms will be available/specified for low power (femto, home) eNBs for residential use. In the end, the effectiveness of ACCS-like algorithms needs to be further proven when taking in consideration more real-life system restrictions following the 3GPP specifications.

7. Conclusion

In this paper the recent advances in project SAMURAI are presented, focusing on the practical and implementability questions of MU-MIMO and CA schemes. This means that the paper shows realistic considerations from hardware implementation point of view, as well as presents performance results under realistic assumptions.

Highlights of current standardisation status in MU MIMO and CA are shown. The interference aware receiver structure for MU MIMO is introduced, with an applicable link to system interfacing solution, that allows the

evaluation of this receiver at system level. System level results are presented, showing that up to 20% gain in cell throughput is achievable by using the interference aware receiver, at the expense of some loss in the cell edge throughput performance. As described in the paper, this receiver algorithm was also implemented in proof of concept hardware platform.

The emulation of the behaviour of multipath fading channel is an important area, for implementing measurement devices enabling the testing of UE and base station elements in realistic circumstances. The work presented in the framework of SAMURAI allows the reproduction of MIMO channel, for subsequent testing and measurement purposes. An important aspect of this work is that it allows the modelling and emulation of channel behaviour taking into account the spatial component of the channel. The results of this work will likely appear in future testing and measurement devices.

Realistic practical investigations of the implementation questions of CA from UE perspective are also shown. Moreover, the study presented in this paper reveals the main issues from testing and measurement point of view, namely in the area of wideband signal generation and spectrum analysis. System level performance results are also presented, revealing that using downlink CA practically doubles UE performance in case of modest load conditions.

One of the most exciting questions is the performance of joint application of MU MIMO and CA transmission schemes in the network. Practical considerations on the implementation issues at the UE, network and test equipment side are analysed in the paper. Besides this qualitative analysis, network level performance curves of both schemes applied jointly are presented. It can be stated that under heavy load conditions applying MU MIMO together with CA compensates for the relatively modest gains that would be achievable by CA only. With applying proper scheduling and adaptive SU/MU MIMO switching, the scheme can provide up to 20% gain in average UE throughput performance, compared to the case when only SU MIMO with CA is used. In the uplink direction, results show that in terms of average user throughput, more than 50% gain is achievable compared to the CA scheme, when CA is extended by multi-cluster scheduling and MU MIMO.

This paper also shows the hardware proof of concept platforms that are (at least partially) direct results of the SAMURAI project. The OpenAirInterface platform was mainly extended by MU MIMO transmission schemes. The ASGARD platform was mostly developed in the framework of the project and is used for implementation of Autonomous Component Carrier Selection algorithm.

Finally, possible future research directions in MU MIMO and CA fields are also pointed out. It can be stated that these future directions, as well as results and main recommendations rising from future research are greatly dependent on the details of schemes that will be part of LTE Release 11 and 12.

8. References & Acknowledgement

[1] Zukang Shen et al, "Overview of 3GPP LTE-advanced carrier aggregation for 4G wireless communications", *IEEE Comm. Mag.*, February 2012, pp. 122-130;

[2] FP7-INFSO-ICT-248268 SAMURAI- Work Package 3: Deliverable D3.2, "Final report on algorithm design and implementation feasibility study", June 2011.

[3] FP7-INFSO-ICT-248268 SAMURAI- Work Package 4: Deliverable D4.2 "Intermediate report on SA schemes and implementation feasibility study", December 2010. FP7 participant restricted.

[4] FP7-INFSO-ICT-248268 SAMURAI – Work Package 4, Deliverable 4.3, "Final report on SA schemes and implementation feasibility study", June 2011.

[5] FP7-INFSO-ICT-248268 SAMURAI – Work Package 4: Deliverable D4.4 "SA schemes implementation report", December 2011.

[6] Q.H. Spence et al, "An Introduction to the Multi User MIMO Downlink", IEEE Comm. Magazine, Oct. 2009;

[7] Jonathan Duplicy, Biljana Badic, Rajarajan Balraj, Rizwan Ghaffar, Péter Horváth, Florian Kaltenberger, Raymond Knopp, István Z. Kovács, Hung T. Nguyen, Deepaknath Tandur and Guillaume Vivier, "MU-MIMO in LTE Systems", EURASIP Journal on Wireless Communications and Networking, vol. 2011, Article ID 496763, 13 pages, 2011. doi:10.1155/2011/496763.

[8] Ghaffar, Rizwan; Knopp, Raymond, "Interference-aware receiver structure for Multi-User MIMO and LTE", EURASIP Journal on Wireless Communications and Networking, Volume 2011: 40.

[9] FP7-INFSO-ICT-248268 SAMURAI- Work Package 2: Deliverable D2.2 "Year 2 System Level Evaluation Report", December 2011. FP7 participant restricted.

[10] FP7-INFSO-ICT-248268 SAMURAI – Work Package 2: Deliverable D2.3 "Final System Level Evaluation Report", October 2012;

[11] FP7-INFSO-ICT-248268 SAMURAI- Work Package 5: Deliverable D5.1 Proof-of-Concept definitions, December 2010. Consortium confidential deliverable.

[12] FP7-INFSO-ICT-248268 SAMURAI – Work Package 5: Deliverable D5.2 "Blocks assessment and system evaluation", October 2012;

[13] http://www.openairinterface.org

[14] http://asgard.lab.es.aau.dk

Other consortium deliverables and main publications are available on www-ict-samurai.eu